Highly efficient homology-directed repair using transient CRISPR/Cpf1-geminiviral replicon in tomato

Tien Van Vu[1,2], Velu Sivankalyani[1], Eun-Jung Kim[1], Mil Thi Tran[1], Jihae Kim[1], Yeon Woo Sung[1], Duong Thi Hai Doan[1], Jae-Yean Kim[1,3,*]

[1]Division of Applied Life Science (BK21 Plus program), Plant Molecular Biology and Biotechnology Research Center, Gyeongsang National University, Jinju 660-701, Republic of Korea.

[2]National Key Laboratory for Plant Cell Biotechnology, Agricultural Genetics Institute, Km 02, Pham Van Dong road, Co Nhue 1, Bac Tu Liem, Ha Noi 11917,Viet Nam.

[3]Division of Life Science (CK1 program), Gyeongsang National University, 501 Jinju-daero, Jinju 52828, Republic of Korea.

*** Correspondence: Jae-Yean Kim (kimjy@gnu.ac.kr)**

ABSTRACT

Genome editing via homology-directed repair (HDR) pathway in somatic plant cells was very inefficient compared to illegitimate repair by non-homologous end joining (NHEJ). Here, compared to a Cas9-based replicon system, we enhanced approximately 3-fold in the HDR-based genome editing efficiency via transient geminiviral replicon system equipping with CRISPR/LbCpf1 in tomato and obtained replicon-free, but with stable HDR alleles. Efficiency of CRISPR/LbCpf1-based HDR was significantly modulated by physical culture conditions such as temperature or light. A ten-day incubation at 31 ^{o}C under light/dark cycles after *Agrobacterium*-mediated transformation performed the best among conditions tested. Further, we developed multi-replicon system which is a novel tool to introduce effector components required for the increase of HDR efficiency. Even if it is still challenging, we also showed a feasibility of HDR-based genome editing without genomic integration of antibiotic marker or any phenotypic selection. Our work may pave a way for transgene-free rewriting of alleles of interest in asexually as well as sexually reproducing plants.

Key words: homology-directed repair (HDR), gene targeting, CRISPR/Cpf1, allele replacement, tomato.

Running title: Advancement of plant HDR by CRISPR/Cpf1

INTRODUCTION

Streptococcus pyogenes CRISPR-associated protein 9 (SpCas9) (Jinek et al., 2012) and *Lachnospiraceae bacterium* Cas12a (LbCas12a or LbCpf1) (Zetsche et al., 2015) have been widely used in genome engineering researches as the guide RNA-enzyme complexes to generate DNA double-stranded breaks (DSBs) in genome of various kingdoms including plantae (Hsu et al., 2014; Barrangou and Doudna, 2016). In plant somatic cells, DSBs are efficiently repaired by a non-homologus end joining (NHEJ) mechanism, which dominates over the homology-directed repair (HDR) pathway (Puchta, 1998; Jiang et al., 2012). NHEJ repair usually leads to different types of mutations including DNA sequence insertion, deletion (Hsu et al., 2014; Zetsche et al., 2015), chromosome rearrangement, or chromosome relocation (Richardson et al., 1998; Ferguson and Alt, 2001; Varga and Aplan, 2005 and our own observations in tomato). To our knowledge, HDR is the major way to precisely edit a gene of interest regardless the mutation types, lengths, and locations of DNA sequences. However, application of HDR in plant has been very limited due to its extremely low efficiency (Puchta, 1998). Therefore, there is a practical demand to develop an efficient HDR-based genome editing system for crop breeding.

Previously, geminiviral replicons combined with the Cas9 or TALEN were successfully used to increase HDR efficiency in tomato (Čermák et al., 2015) but the efficiency might not be high enough for practical applications in crop plant improvement (Hummel et al., 2018). It was suggested that Cpf1 might have an advantage in HDR-based genome editing compared to Cas9, because the cutting site of Cpf1 is located distal to the core target sequence and the protospacer adjacent motif (PAM), allowing recutting even after indel mutations introduced during NHEJ-mediated repair (Baltes et al., 2014). We hypothesized that combination of a CRISPR/Cpf1 complex and a *de novo* engineered geminiviral replicon could be able to overcome the barrier in plant HDR.

Here, we report an efficient homology-directed repair using transient CRISPR/LbCpf1-geminiviral replicon in tomato. Through this work we aimed to level up HDR efficiency for practical applications in crop plant breeding.

RESULTS AND DISCUSSION

CRISPR/LbCpf1-based geminiviral replicon system highly enhanced HDR in tomato

To test the hypothesis, we re-engineered a *Bean Yellow Dwarf Virus* (*BeYDV*) replicon to supply high doses of homologous donor templates, and used a CRISPR/LbCpf1 system (Zetsche et al., 2015) for DSB formation (Figure 1A and 1B). Selection of HDR events was supported by a double selection/screening system using kanamycin resistance and anthocyanin overproduction (Figure 1A).

To validate our system, the LbCpf1 expression cassette driven by a CaMV 35S promoter and 5'UTR with AtUBI10 intron I, guide RNA scaffolds and donor templates were cloned into the *de novo* engineered geminiviral DNA amplicon (Figure 1B**)** and transformed via Agrobacteria into tomato cotyledon explants. The *de novo* engineered geminiviral DNA amplicon system exhibited efficient and durable maintenance of circularized DNAs in tomato leaves (Supplemental Figure 1). The LbCpf1 system using two guide RNAs for targeting the ANT1 gene, a key transcription factor controlling anthocyanin pathway, showed the much higher HDR efficiency, at 4.51±0.63 %, visible as purple calli and/or shoots (Figure 1C and 1D), compared to the other control constructs including a "minus Rep" (pRep$^-$), "minus gRNA" (pgRNA$^-$), and comparable to a CRISPR/SpCas9-based construct (pTC217). The data revealed that functional geminiviral replicons were crucial for the enhancement of HDR efficiencies (Figure 1C) as shown in other works (Čermák et al., 2015). This is the first report showing highly efficient HDR in plants using Cas12a expressing from a geminiviral replicon.

Light conditions or photoperiods enhanced HDR efficiency of CRISPR/LbCpf1 system

Boyko and coworkers (2005) showed the strong impact of short-day conditions on intrachromosomal recombination repair (ICR) in *Arabidopsis*. We tested if the same could be true in tomato somatic cells. Using various lighting regimes, including complete darkness (DD), short (8-h light/16-h dark; 8L/16D) and long (16L/8D) day conditions, we found that HDR efficiencies achieved under short and long day conditions were higher than those in the DD condition in the case of LbCpf1, but not SpCas9, and reached up to 6.62±1.29% ($p<0.05$, Figure 1E). The advancement of LbCpf1-based HDR system might be explained by stress-

responses of the host cells which rushed for maintenance of genome stability (Boyko et al., 2005) by any means of DNA repairs including HDR.

CRISPR/LbCpf1-based HDR was significantly higher compared to CRISPR/Cas9-based system at high temperature

Temperature is an important factor controlling ICR (Boyko et al., 2005) and CRISPR/Cas9-based targeted mutagenesis in plants (LeBlanc et al., 2018) and CRISPR/Cpf1-based HDR through controlling genome accessibility in zebrafish and *Xenopus* (Moreno-Mateo et al., 2017) were also reported. Pursuing the approach for improvement of HDR, we compared HDR efficiencies of pHR01 and pTC217 systems at various temperature treatments, since the two nucleases, SpCas9 and LbCpf1 may respond differently. Our data revealed that within the temperature range of 19-31^{o}C, somatic HDR increased with increasing temperature (Figure 1F). Notably, at 31^{o}C, LbCpf1 showed more than 2-fold higher HDR efficiency compared to SpCas9 ($p<0.05$). The results supported the principle of stress-stimulated HDR in plants reported by Boyko and coworkers (2005). The ease of genome accessibility at high temperatures of LbCpf1 (Moreno-Mateos et al., 2017) in combination with the ability to repeatedly cut at the target sites (Zetche et al., 2015) may explained higher HDR efficiencies of LbCpf1 compared to that of SpCas9. For the first time comparison data of plant HDR between Cas9 and Cpf1-based systems are shown, offering an alternatively better system for plant HDR improvement.

A multiple replicon system performed better for HDR than the single one

To compete with the efficient NHEJ pathway, protein involving in the HDR pathway were over-expressed, activated or enhanced leading to significant higher efficiencies (Ye et al., 2018; Pawelczak et al., 2018). For further improvement of our system, we used several molecular approaches for HDR improvement in tomato. The first was to activate nine HDR pathway genes (Supplemental Table 1) using the dCas9-sun tag/scFv-VP64 activation system (Tanenbaum et al., 2014). A single construct system (pHR01-Activ, Supplemental Figure 2A) showed negative effects on HDR (data not shown), which may be due to its large size (~32 kb as T-DNA and ~27 kb as circularized replicon).

The size of viral replicons is inversely correlated with their copy numbers (Suarez-Lopez and Gutierrez, 1997; Baltes et al., 2014). In this work we also tested a novel idea to use a T-DNA producing multiple replicons (pHR01-MR, Figure 2A, and Supplemental Figure 2B). Compared to pHR01, the construct showed HDR efficiencies with 39% increase. We also confirmed the release of three replicons from a single vector (pHR01-MR) used in this work (Figure 2B). To our best knowledge, this is the first report that multiple replicons can be used for efficient genome editing via HDR pathway. This multiple replicon system may also provide more flexible choices for expressing multiple genes/genetic tools/DNA agents with high copies in plant cells.

The true HDR events were obtained at high frequency

To verify the HDR repair events in the study, PCR analyses were conducted using primers specific for the right (UPANT1-F1/NptII-R1) and left (ZY010F/TC140R) (Figure 1A; Supplemental Table 2 and 3) junctions, using genomic DNAs extracted from derived HDR events (independently regenerated purple plants or Genome Edited generation 0 (GE0)) (Fig 2C, Supplemental Figure 3). For pHR01, all (16/16) of the independent events the expected band for right junction integration and 10/16 independent events showed the expected band for left junction repair (Figure 2B). More importantly, 15 out 16 events showed no amplification of circularized forms (Supplemental Figure 4) of the DNA replicon, and even the replicon-carrying event lost it after long-term growth in greenhouse conditions (data not shown), indicating those plants were free of replicon (Figure 2D). The loss of replicon might be explained by a reversed construction of the donor template (Figure 1B) leading to opposite arrangement of LIR forward promoter sequence against a 35S promoter sequence (LIR-p35S orientation interference) and thus triggering silencing mechanism in the plant cells in later stage, especially when antibiotic selection pressure was absent. This explanation was later confirmed by the appearance of replicons in majority of plants regenerated using other replicon systems absented the LIR-p35S orientation interference. The PCR products were sequenced to identify junction sequences. A majority of the events (11/16) showed sequences corresponding to perfect right arm integration by HDR repair, 5/16 events showed a combination of HDR and NHEJ repair with NHEJ fingerprint at the 5' terminal of pNOS sequence (Supplemental Figure 5A), highlighted in blue in the event C1.8). All of the

sequences amplified from left junctions showed perfected DNA sequence exchange by HDR pathway (Supplemental Figure 5B).

The HDR allele was stably inherited in offspring by self-pollination as well as backcrossing

To confirm stable heritable edits, we grew Genome Edited generation 1 (GE1) plants (Figure 2E) obtained from self-pollination of LbCpf1-based HDR GE0 events, and found segregating population in purple phenotype (Supplemental Table 4) similar to data shown by Čermák and coworkers (2015). PCR analyses of the segregated plants showed inheritance of the edited allele (Figure 2F and Supplemental Figure 6). Offspring segregated from the #C1.4 event were analyzed in detail. Five dark-purple plants (C1.4.1-C1.4.5, were homozygous for the ANT1 HDR edited allele, Supplemental Figure 7), six pale purple plants (C1.4.30-C1.4.35, were heterozygous for the ANT1 HDR edited allele, Supplemental Figure 7), and two wild-type like plants did not contain the HDR edited allele, as expected (Figure 2F, predicted results correlating to their phenotypes). Dark-purple plants showed the PCR amplification from the replaced allele, but no amplification of wild-type allele when PCRs were performed using primers flanking outside the editing site (Figure 1A). In contrast, heterozygous and wild-type plants showed a band corresponding to the wild-type allele. Further assessment indicated that the GE2 offspring of the homozygous GE1 were all dark purple and their back-crossed (to WT female as pollen acceptors) BC1F1 generation showed all pale purple phenotype (Supplemental Figure 7**)**. Sanger sequencing revealed perfect inheritance of the HDR edited allele from GE0 generation of event C1.4 (Supplemental Figure 8) to its homozygous offspring. These data also showed no amplification of circular forms of the DNA replicon (Figure 2F and Supplemental Figure 6) indicating that GE1 plants were also free of the replicons. By contrast, Several GE1 plants obtained from the pTC217 showed amplification of circularized replicons (Supplemental Figure 5B, data not shown). It is worthy note that the pTC217 vector arrangement (Figure 1B) is in the absence of the LIR-p35S orientation interference.

Practically successful editing by HDR of a HKT1;2 allele

To show the applicability of our HDR system in practical plant genome editing we sought to use it to edit a potentially agronomical trait and thus salinity tolerance was chosen. The High-affinity K^+ Transporter 1;2 (HKT1;2) plays important role in the maintenance of K+ uptake under salt stress (Ali et al., 2012). The salinity tolerance was shown to be determined by a single N/D variance (N217D in tomato) in the pore region of HKT1;2, which determines the selectivity for Na+ and K+ (Ali et al., 2016). We succeeded to have a perfect HDR GE0 event to produce the salt tolerant allele (N217D) (Ali et al., 2016) (Figure 3A, Supplemental Table 5) using our system with a *HKT1;2* gene donor template which contains neither antibiotic selection marker nor ANT1 color marker (Figure 3B). The CRISPR/LbCpf1 system was very effective for NHEJ repair as it generated up to 72% indel mutation rates (Supplemental Figure 9). The edited event with the D217 allele shows normal morphology compared to WT (Figure 3C). It should be noted that the mutated nucleotide (A to G) of *HKT1;2* is not accessible by any currently known base editor (BE) including xCas9-ABE (Hu et al., 2018), underlining the significance of HDR-based genome editing.

Taken together, through applications of various approaches, our study showed a high improvement of HDR efficiency in tomato somatic cells. The HDR allele exhibited similar inheritance to natural allele as it was transferred to next generation following Mendelian rules. The advancement of HDR in somatic cells and obtaining replicon-free HDR-edited plants in GE0 generation will open a door for practical applications of the technique to genetically improve crop traits, with special interest in asexually reproducing crops.

MATERIAL AND METHODS

Construction and cloning of HDR testing systems

The entire design principle and cloning works followed MoClo (Weber et al., 2011) and Golden Gate (Engler et al., 2014) protocols. The pLSL.R.Ly was designed by amplifying the long intergenic region (LIR), short intergenic region (SIR) and lycopene marker from pLSLR plasmid (Čermák et al., 2015) and cloned following the order shown in the Supplemental Figure 1A. Level 2 Golden Gate BpiI restriction sites flanking the pink marker gene (lycopene) were also integrated inside the replicon for cloning of HDR expression cassettes. The release of circularized DNA replicons was validated in tomato leaves (Supplemental Figure 1B) as

well as tomato cotyledon explants (data not shown). pTC147 and pTC217 plasmids (Čermák et al., 2015) were obtained from Addgene and was used as a reference. The LbCpf1-based HDR replicons were similarly designed and cloned (as the SpCas9-based constructs) with two guide RNAs (LbCpf1_gRNA1 and LbCpf1_gRNA2, Figure 1A). Donor DNAs were constructed for integration of an antibiotic selection marker (NptII) and insertion of a CaMV 35S promoter for driving over-expression of ANT1 gene (Figure 1A). The dual guide RNA construct was designed by multiplexing the LbCpf1 crRNAs as a tandem repeat of scaffold RNA followed by 23nt guide RNA sequences. The crRNAs were driven by an AtU6 promoter (Kamoun Lab, Addgene #46968) and terminated by a 7-T chain sequences.

Tomato transformation

Our research study on HDR improvement was conducted using tomato (Hongkwang cultivar, a local variety) as a model plant. All the binary vectors were transformed into *Agrobacterium tumefaciens* GV3101 (pMP90) using electroporation. Agrobacterium-mediated transformation was used to deliver editing tools into tomato cotyledon fragments (Supplemental Figure 10). Explants for transformation were prepared from 7-day-old cotyledons. Sterilized seeds of the Hongkwang cultivar were grown in MSO medium (half-strength MS medium containing 30 g/L of sucrose, pH 5.8) at 25±2ºC under 16 h/8 h light/dark conditions. Seven-day-old seedlings were collected, and their cotyledonary leaves were sliced into 0.2-0.3 cm fragments. The fragments (explants) were pre-treated on PREMC medium [MS basal salts, Gamborg B5 vitamins, 2.0 mg/L of Zeatin trans-isomer and 0.2 mg/L of indolyl acetic acid (IAA), 1 mM of putrescine and 30 g/L of glucose, pH 5.7] for 1 day. The pre-cultured explants were then pricked and transformed using *A. tumefaciens* GV3101::pMP90 cells carrying HR construct(s).

A. tumefaciens GV3101::pMP90 cells were grown in primary culture overnight (LB containing suitable antibiotics) in a shaking incubator at 30ºC. Agrobacteria were then collected from the culture (OD 0.6-0.8) by centrifugation. The cells were re-suspended in liquid ABM-MS (pH 5.2) and acetosyringone 200 µM. Transformation was carried out for 25 min at RT. The explants were then transferred to co-cultivation medium containing all of the components in the ABM-MS medium and acetosyringone 200 µM, pH 5.8. The co-cultivation plates were kept in the darkness at 25ºC for 2 days, and the explants were shifted to non-selection medium (NSEL) for 5 days and then sub-cultured to selection medium (SEL5). The

non-selection and selection media contained all of the components in the pre-culture medium, as well as 300 mg/L of timentin and 80 mg/L of kanamycin. Sub-culture of the explants was carried out at 14-day-interval to achieve the best regeneration efficiency. Explants containing purple calli or shoots were then transfer onto SEL5R medium (similar to SEL5 but reduced zeatin trans-isomer to 1.0 mg/L) for further regeneration and/or elongation. When the shoots were sufficiently long (1.5-3.0 cm), they were transferred to rooting medium (containing all of the components in the elongation medium except zeatin trans-isomer and plus 1.0 mg/L IBA) to generate intact plants. The intact plants from the rooting medium were transferred to vermiculite pots to allow them to harden before shifting them to soil pots in a greenhouse with a temperature of 26±2ºC and under a 16 h/8 h photoperiod. Experimental treatment of physical conditions and data collection were conducted as described in Supplemental Figure 10.

HDR event evaluation

Assessment of gene targeting junctions was performed by conventional PCR using primers flanking left (UPANT1-F1/NptII-R1) and right (ZY010F/TC140R (Cermak et al., 2015) Supplemental Table 2 and 3) junctions and a high fidelity taq DNA polymerase (Phusion taq, Thermo Fisher Scientific, USA) and Sanger sequencing (Solgent, Korea). DNA amplicons were evaluated by semi-quantitative PCRs and qPCRs (using KAPA SYBR FAST qPCR Kits, Sigma-Aldrich, USA). Analyses of inherited behaviors of HDR edited allele were performed with genome edited generation 1 (GE1) by PCRs and Sanger sequencing. Circularized replicons were detected using PCR with the respected primers for either pHR01 (Supplemental Table 2) or pTC217 (Supplemental Table 3).

Statistical analyses

HDR efficiencies were recorded in at least three replicates and statistically analyzed and plotted using PRISM 7.01 software. In Figure 1C, multiple comparisons of the HDR efficiencies of the other constructs with that of pRep^{-} were done by one-way ANOVA analysis (Uncorrected Fisher LSD test, n=3, df=2, t=4.4; 4.4 and 1.5 for pTC217; pHR01 and pgRNA^{-}, respectively). In Figure 1E, pairwise comparisons of the HDR efficiencies of pTC217 and pHR01 in the three lighting conditions were done by Student t-test (DD: t=1.222, df=4; 8L/16D: t=2.424,

df=7 and 16L/8D: t=3.059, df=4). In Figure 1F, comparisons of the HDR efficiencies of pTC217 and pHR01 in the various temperature conditions were done by Student t-test (19^{o}C: t=2.656, df=2; 25^{o}C: t=3.346, df=2; 28^{o}C: t=2.099, df=5; 31^{o}C: t=4.551, df=2).

FUNDING

This work was supported by the National Research Foundation of Korea (Grant NRF 2017R1A4A1015515) and by the Next-Generation BioGreen 21 Program (SSAC, Grant PJ01322601), Rural Development Administration (RDA), Republic of Korea.

AUTHOR CONTRIBUTIONS

T.V.V., V.S. and J.Y.K. designed the experiments; T.V.V., V.S., E, J. K., M.T.T., J.K., Y.W.S., and D.T.H.D performed the experiments; T.V.V. and J.Y.K. analyzed the results; T.V.V. and J.Y.K. wrote the manuscript.

COMPETING INTERESTS

The authors have submitted a Korean patent application (application no. 10-2018-0007579) based on the results reported in this paper.

ACKNOWLEDGMENTS

We thank MinWoo Park for providing Hongkwang tomato seeds.

REFERENCES

Ali, A., Raddatz, N., Aman, R., Kim, S., Park, H.C., Jan, M., Baek, D., Khan, I.U., Oh, D.H., Lee, S.Y., et al. (2016) A Single Amino-Acid Substitution in the Sodium Transporter HKT1 Associated with Plant Salt Tolerance. Plant Physiol. 171(3):2112-2126.

Ali, Z., Park, H.C., Ali, A., Oh, D.H., Aman, R., Kropornicka, A., Hong, H., Choi, W., Chung, W.S., Kim, W.Y., et al. (2012). TsHKT1;2, a HKT1 homolog from the extremophile Arabidopsis relative Thellungiella salsuginea, shows K(+) specificity in the presence of NaCl. Plant Physiol. 158(3):1463-1474.

Baltes, N.J., Gil-Humanes, J., Cermak, T., Atkins, P.A. and Voytas, D.F. (2014). DNA replicons for plant genome engineering. Plant Cell. 26(1):151-163.

Barrangou, R. and Doudna, J.A. (2016). Applications of CRISPR technologies in research and beyond. Nat Biotechnol. 34(9):933-941.

Boyko, A., Filkowski, J. and Kovalchuk, I. (2005). Homologous recombination in plants is temperature and day-length dependent. Mutat Res. 572(1-2):73-83.

Čermák, T., Baltes, N.J., Čegan, R., Zhang, Y. and Voytas, D.F. (2015). High-frequency, precise modification of the tomato genome. Genome Biol. 16:232.

Engler, C., Youles, M., Gruetzner, R., Ehnert, T.M., Werner, S., Jones, J.D., Patron, N.J. and Marillonnet, S. (2014). A golden gate modular cloning toolbox for plants. ACS Synth Biol. 3(11):839-843.

Ferguson, D.O. and Alt, F.W. (2001). DNA double strand break repair and chromosomal translocation: lessons from animal models. Oncogene. 20(40):5572-5579.

Hsu, P.D., Lander, E.S., and Zhang, F. (2014). Development and applications of CRISPR-Cas9 for genome engineering. Cell. 157(6):1262-1278.

Hu, J.H., Miller, S.M., Geurts, M.H., Tang, W., Chen, L., Sun, N., Zeina, C.M., Gao. X., Rees, H.A., Lin, Z. and Liu, D.R. (2018). Evolved Cas9 variants with broad PAM compatibility and high DNA specificity. Nature. 556(7699):57-63.

Hummel, A.W., Chauhan, R.D., Cermak, T., Mutka, A.M., Vijayaraghavan, A., Boyher, A., Starker, C.G., Bart, R., Voytas, D.F. and Taylor, N.J. (2018). Allele exchange at the EPSPS locus confers glyphosate tolerance in cassava. Plant Biotechnol J. 16(7):1275-1282.

Jiang, W., Zhou, H., Bi, H., Fromm, M., Yang, B. and Weeks, D.P. (2013). Demonstration of CRISPR/Cas9/sgRNA-mediated targeted gene modification in Arabidopsis, tobacco, sorghum and rice. Nucleic Acids Res. 41(20):e188.

Jinek, M., Chylinski, K., Fonfara, I., Hauer, M., Doudna, J.A., and Charpentier, E. (2012). A programmable dual-RNA-guided DNA endonuclease in adaptive bacterial immunity. Science. 337(6096):816-821.

LeBlanc, C., Zhang, F., Mendez, J., Lozano, Y., Chatpar, K., Irish, V.F. and Jacob, Y. (2018). Increased efficiency of targeted mutagenesis by CRISPR/Cas9 in plants using heat stress. Plant J. 93(2):377-386.

Moreno-Mateos, M.A., Fernandez, J.P., Rouet, R., Vejnar, C.E., Lane, M.A., Mis, E., Khokha, M.K., Doudna, J.A. and Giraldez, A.J. (2017). CRISPR-Cpf1 mediates efficient homology-directed repair and temperature-controlled genome editing. Nat Commun. 8(1):2024.

Pawelczak, K.S., Gavande, N.S., VanderVere-Carozza, P.S., Turchi, J.J. (2018). Modulating DNA Repair Pathways to Improve Precision Genome Engineering. ACS Chem Biol. 13(2):389-396.

Puchta, H. (1998). Repair of genomic double-strand breaks in somatic plant cells by one-sided invasion of homologous sequences. The Plant Journal 13(3):331–339.

Richardson, C., Moynahan, M.E. and Jasin, M. (1998). Double-strand break repair by interchromosomal recombination: suppression of chromosomal translocations. Genes Dev. 12(24):3831-3842.

Suárez-López, P. and Gutiérrez, C. (1997). DNA replication of wheat dwarf geminivirus vectors: effects of origin structure and size. Virology. 227(2):389-399.

Tanenbaum, M.E., Gilbert, L.A., Qi, L.S., Weissman, J.S. and Vale, R.D. (2014). A protein-tagging system for signal amplification in gene expression and fluorescence imaging. Cell. 159(3):635-646.

Varga, T. and Aplan, P.D. (2005). Chromosomal aberrations induced by double strand DNA breaks. DNA Repair (Amst). 4(9):1038-1046.

Weber, E., Engler, C., Gruetzner, R., Werner, S. and Marillonnet, S. (2011). A modular cloning system for standardized assembly of multigene constructs. PLoS One. 6(2):e16765.

Ye, L., Wang, C., Hong, L., Sun, N., Chen, D., Chen, S., Han, F. (2018). Programmable DNA repair with CRISPRa/i enhanced homology-directed repair efficiency with a single Cas9. Cell Discov. 4:46.

Zetsche, B., Gootenberg, J.S., Abudayyeh, O.O., Slaymaker, I.M., Makarova, K.S., Essletzbichler, P., Volz, S.E., Joung, J., van der Oost, J., Regev, A., et al. (2015). Cpf1 is a single RNA-guided endonuclease of a class 2 CRISPR-Cas system. Cell. 163(3):759-771.

FIGURE LEGENDS

Figure 1. HDR-based genome editing of ANT1 locus.

(**A**) Representatives of ANT1 targeting sites and homologous DNA donor template construction. The upstream sequence of ANT1 locus (middle panel) was selected for targeting by HDR. Two guide RNAs were used (depicted by two vertical arrows on the middle panel and sequence details in bottom panel). Kanamycin expression cassette (pNOS-NptII-tOCS) and CaMV 35S promoter was designed to be inserted at a position 142 bp upstream of ANT1 start codon.

(**B**) T-DNA constructs used for HDR improvement experiments. The dual guide RNA scaffold (2x1gRNA^{ANT1}) was driven by Arabidopsis U6 promoter core element (75bp). LbCpf1 expression cassette was re-engineered to contain Arabidopsis Ubiquitin 1 intron I downstream of CaMV 35S promoter and upstream of LbCpf1 and to be terminated by CaMV 35S terminator (35S-LbCpf1I-t35S). Red and orange boxes show long intergenic region and short intergenic region of geminivirus DNA.

(**C**) HDR efficiency comparison among different constructs.

(**D**) Representative photograph of HDR edited T0 events indicating as purple calli (red arrows) or direct HDR shoot formation (purple arrow).

(**E**) Impact of photoperiod on HDR. Tomato cotyledon fragments transformed were incubated under different lighting regimes for the first 10 days post-washing. DD: continuous darkness; 8L/16D: 8 hours-lighting/16 hours-darkness; 16L/8D: 16 hours-lighting/8 hours-dark.

(**F**) HDR efficiencies of pTC217 and pHR01 construct obtained in various temperatures. HDR efficiencies were recorded in at least triplicates, calculated and plotted using PRISM 7.01 software (details of statistical analyses are described in Methods section). *: significantly different ($p<0.05$); ns: not significantly different; p values are showing on the top of the bars of (**F**) for comparisons.

Data in (**B**), (**E**) and (**F**) are represented as mean ± SEM.

Figure 2. Novel approaches for HDR improvement and analyses of the HDR edited plants.

(**A**) Multi-replicon construct tested for improvement of HDR over NHEJ. Red and orange boxes show long intergenic region and short intergenic region of geminivirus DNA.
(**B**) PCR detection of circularized replicons simultaneously released from multiple replicon vector (pHR01-MR). 0d, 3d, 6d and 9d: samples collected at 0, 3, 6 and 9 days post transformation with *Agrobacterium* carrying pHR01-MR.
(**C**) Representative HDR edited plant in greenhouse conditions and their fruits.
(**D**) PCR analysis data of some representative HDR independent events.
(**E**) Generation 1 of the HDR edited events (GE1). GE1 plant (left) germinated in soil pot in comparison with wild-type plant (right).
(**F**) PCR analysis data of some GE1 offspring of C1.4 event. P: pHR01 plasmid isolated from Agrobacteria; L: 1kb ladder; N: water control; WT: wild-type tomato Hongkwang; C1.1, C1.2, C1.3, C1.8: Independent LbCpf1-based HDR GE0 events; C1.4.1, C1.4.2, C1.4.3, C1.4.4 and C1.4.5: GE1 plants, showing dark purple color, obtained from self-pollination of the event C1.4.

Figure 3. HKT1;2 N217D allele editing by HDR using the CRIPSR/Cpf1-based replicon system.

(**A**) Sanger sequencing of the event #C156 showing perfectly edited HKT1;2 N217 to D217 allele with WT allele as a reference. The nucleotides highlighted in the discontinuous red boxes denote intended modifications for N217D; PAM and core sequences (to avoid re-cutting).
(**B**) HDR construct layout for HKT1;2 editing. There is neither selection nor visible marker integrated into the donor sequence. The *Npt*II marker was used for enrichment of transformed cells.
(**C**) Morphology of the HKT1;2 N217D edited event compared to its parental WT in greenhouse conditions.

LIST OF SUPPLEMENTAL TABLES

Supplemental Table 1. Targeted genes and guide RNAs used in HDR activation experiment.

Supplemental Table 2. Primers for LbCpf1-based HR event analyses

Supplemental Table 3. Primers for SpCas9-based HR event analyses

Supplemental Table 4. Phenotypic segregation of self-pollinated offspring of the LbCpf1-based HDR events

Supplemental Table 5. Summary of *SlHKT1;2* HDR experiment

LIST OF SUPPLEMENTAL FIGURES

Supplemental Figure 1. The *de novo* engineered geminiviral amplicon (named as pLSL.R.Ly) and its replication in tomato.

(**A**) Map of pLSL.R.Ly. The DNA amplicon is defined by its boundary sequences (Long Intergenic Region, LIR) and a terminated sequence (Short Intergenic Region, SIR). The replication associated protein (Rep/RepA) is expressed from the LIR promoter sequence. All of the expression cassettes of HDR tools were cloned into the vector by replacing the red marker (Lycopene) using a pair of type IIS restriction enzyme (BpiI, flanking ends are TGCC and GGGA). Left (LB) and right (RB) denote the borders of a T-DNA.
(**B**) Circularized DNA detection in tomato leaves infiltrated with pLSL.R.Ly compared to that of pLSLR. Agrobacteria containing the plasmids were infiltrated into tomato leaves (Hongkwang cultivar) and infiltrated leaf were collected at 6, 8 and 11 dpi and used for detection of circularized DNAs. N: water; P1: positive control for pLSL.R.Ly; positive control for P2: pLSLR; Cx: Control samples collected at x dpi; Ixy: infiltrated sample number y collected at x dpi; I11V: sample collected from leaves infiltrated with pLSLR at 11 dpi. PCRs using primers specific to GAPDH were used as loading control.

Supplemental Figure 2 Novel systems for HDR improvement.

(**A**). Single construct system for activation of HDR-related genes involving in HDR repair pathway. Long intergenic region (LIR) and short intergenic region (SIR) are depicted by color bars in the bottom.
(**B**). Schematic system and released forms of multiple replicon system. General construction of multiple replicon complex is designed with 3 LIR and 3 SIR sequences (top panel). Donor template was cloned in one replicon and the other component for inducing DSBs were placed in

423 the other replicon (middle panel). Three replicons would be formed from the construct (bottom
424 panel).

425 **Supplemental Figure 3. Morphological appearance of GE0 plants**

426 **Supplemental Figure 4. Circularized DNA replicon released by HDR vectors.**

427 (**A**) pHR01 replicon.
428 (**B**) pTC217 replicon.

429 **Supplemental Figure 5. Sanger sequencing data to confirm donor exchanges.**

430 (**A**) Right junction.

431 (**B**) Left junction. C1.1, C1.2, C1.3, C1.8, C1.11, C1.12, and C1.17: Independent LbCpf1-based
432 HDR GE0 events

433 **Supplemental Figure 6. PCR analyses of GE1 plants obtained from GE0 LbCpf1-based HR**
434 **events.**

435 P: pHR01 plasmid isolated from Agrobacteria; L: 1kb ladder; N: Water control; WT: wild-type
436 Hongkwang; C1.6.1-C1.6.5: GE1 offspring of event C1.6.; C1.9.1: GE1 offspring of event C1.9;
437 C1.10.1 and C1.10.2: GE1 offspring of event C1.10; C1.11.1-C1.11.4: GE1 offspring of event
438 C1.11; C1.12.1-C1.12.5: GE1 offspring of event C1.12; C1.14.1-C1.14.4: GE1 offspring of
439 event C1.14; C1.15.1 and C1.15.2: GE1 offspring of event C1.15; C1.16.1-C1.16.4: GE1
440 offspring of event C1.16.

441 **Supplemental Figure 7. Morphological appearance of GE1 plants**

442 **Supplemental Figure 8. Analyses of left and right junction sequences of GE1 plants.**

443 Sanger sequencing data to confirm donor exchanges for right (**A**) and left (**B**) junctions of the
444 GE1 plants are presented.

445 **Supplemental Figure 9. Alignment of targeted regions isolated from the HKT12 events.**

18/25 events (highlighted in yellow) showed strong double peaks indicating single/bi-allelic mutations. 6/25 events showed clearly bi-allelic mutations. C77 showed weak (30%) double peaks. C83 and C105 showed large truncations.

Supplemental Figure 10. Timeline and contents of *Agro*-mediated transformation protocol used in this work.

Step by step protocol is presented with each number in the circles indicates number of days after seed sowing (upper panel) and treatments used in each steps are shown in below panel.

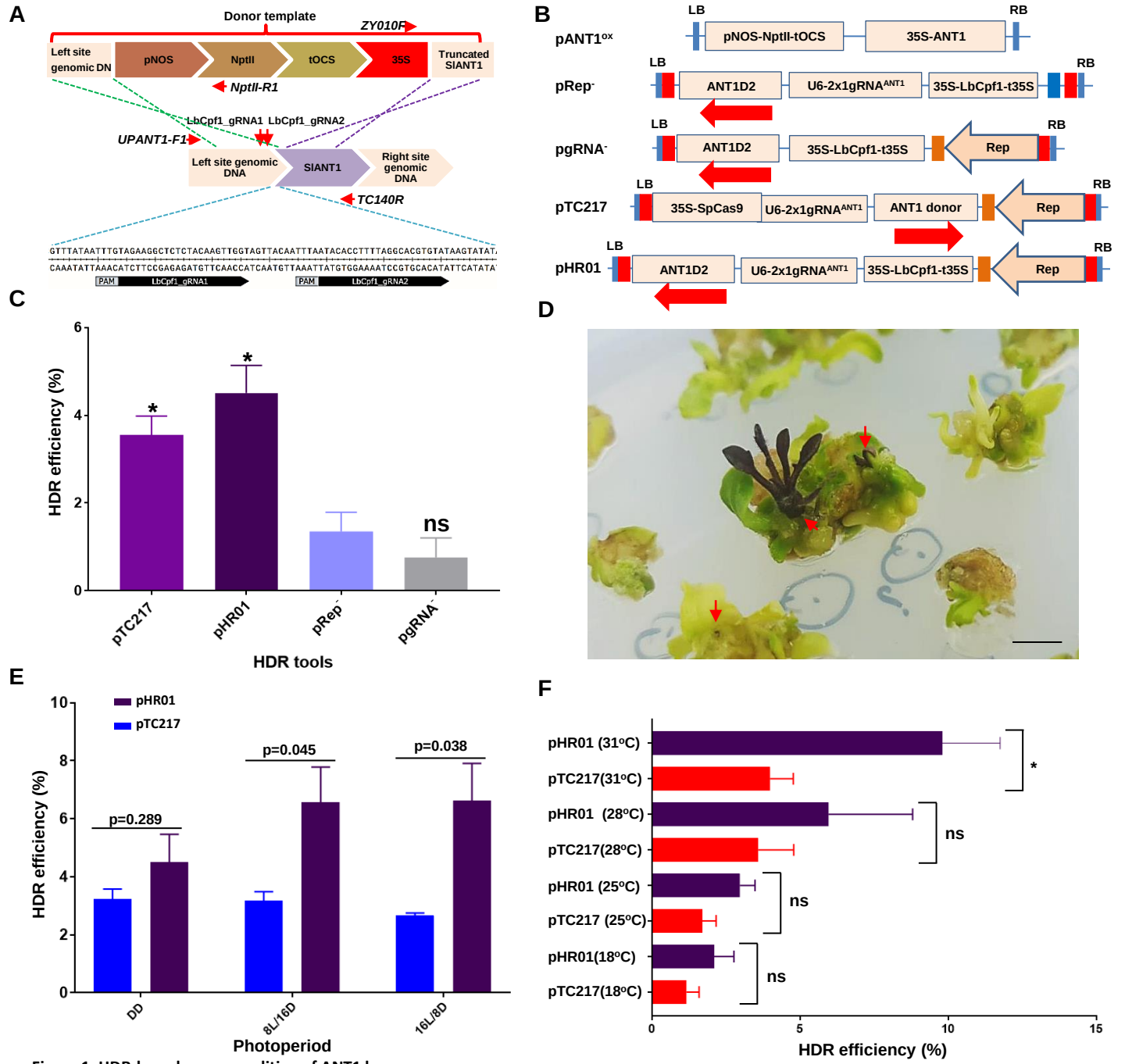

Figure 1. HDR-based genome editing of ANT1 locus.

(**A**) Representatives of ANT1 targeting sites and homologous DNA donor template construction. The upstream sequence of ANT1 locus (middle panel) was selected for targeting by HDR. Two guide RNAs were used (depicted by two vertical arrows on the middle panel and sequence details in bottom panel). Kanamycin expression cassette (pNOS-NptII-tOCS) and CaMV 35S promoter was designed to be inserted at a position 142 bp upstream of ANT1 start codon.

(**B**) T-DNA constructs used for HDR improvement experiments. The dual guide RNA scaffold (2x1gRNA^{ANT1}) was driven by Arabidopsis U6 promoter core element (75bp). LbCpf1 expression cassette was re-engineered to contain Arabidopsis Ubiquitin 1 intron I downstream of CaMV 35S promoter and upstream of LbCpf1 and to be terminated by CaMV 35S terminator (35S-LbCpf1I-t35S). Red and orange boxes show long intergenic region and short intergenic region of geminivirus DNA.

(**C**) HDR efficiency comparison among different constructs.

(**D**) Representative photograph of HDR edited T0 events indicating as purple calli (red arrows) or direct HDR shoot formation (purple arrow). Scale bar = 5 mm.

(**E**) Impact of photoperiod on HDR. Tomato cotyledon fragments transformed were incubated under different lighting regimes for the first 10 days post-washing. DD: continuous darkness; 8L/16D: 8 hours-lighting/16 hours-darkness; 16L/8D: 16 hours-lighting/8 hours-dark.

(**F**) HDR efficiencies of pTC217 and pHR01 construct obtained in various temperatures. HDR efficiencies were recorded in at least triplicates, calculated and plotted using PRISM 7.01 software (details of statistical analyses are described in Material and Methods section). *: significantly different ($p<0.05$); ns: not significantly different; p values are showing on the top of the bars of (**F**) for comparisons.

Data in (**B**), (**E**) and (**F**) are represented as mean ± SEM.

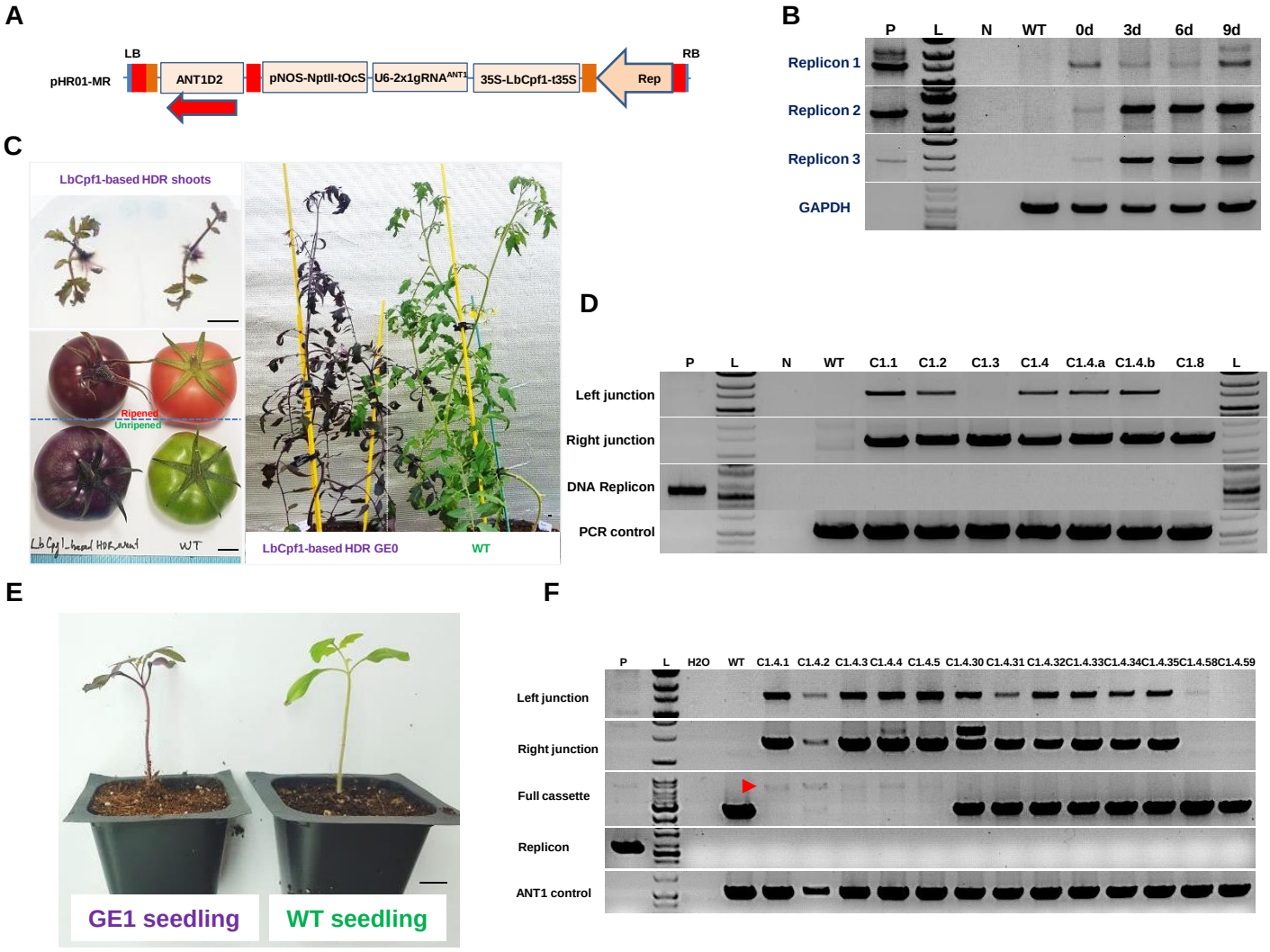

Figure 2. Novel approaches for HDR improvement and analyses of the HDR edited plants.

(**A**) Multi-replicon construct tested for improvement of HDR over NHEJ. Red and orange boxes show long intergenic region and short intergenic region of geminivirus DNA.

(**B**) PCR detection of circularized replicons simultaneously released from multiple replicon vector (pHR01-MR). 0d, 3d, 6d and 9d: samples collected at 0, 3, 6 and 9 days post transformation with *Agrobacterium* carrying pHR01-MR.

(**C**) Representative HDR edited plant in greenhouse conditions and their fruits. Scale bars = 1 cm.

(**D**) PCR analysis data of some representative HDR independent events.

(**E**) Generation 1 of the HDR edited events (GE1). GE1 plant (left) germinated in soil pot in comparison with wild-type plant (right). Scale bar = 1 cm.

(**F**) PCR analysis data of some GE1 offspring of C1.4 event. P: pHR01 plasmid isolated from Agrobacteria; L: 1kb ladder; N: water control; WT: wild-type tomato Hongkwang; C1.1, C1.2, C1.3, C1.8: Independent LbCpf1-based HDR GE0 events; C1.4.1, C1.4.2, C1.4.3, C1.4.4 and C1.4.5: GE1 plants, showing dark purple color, obtained from self-pollination of the event C1.4.

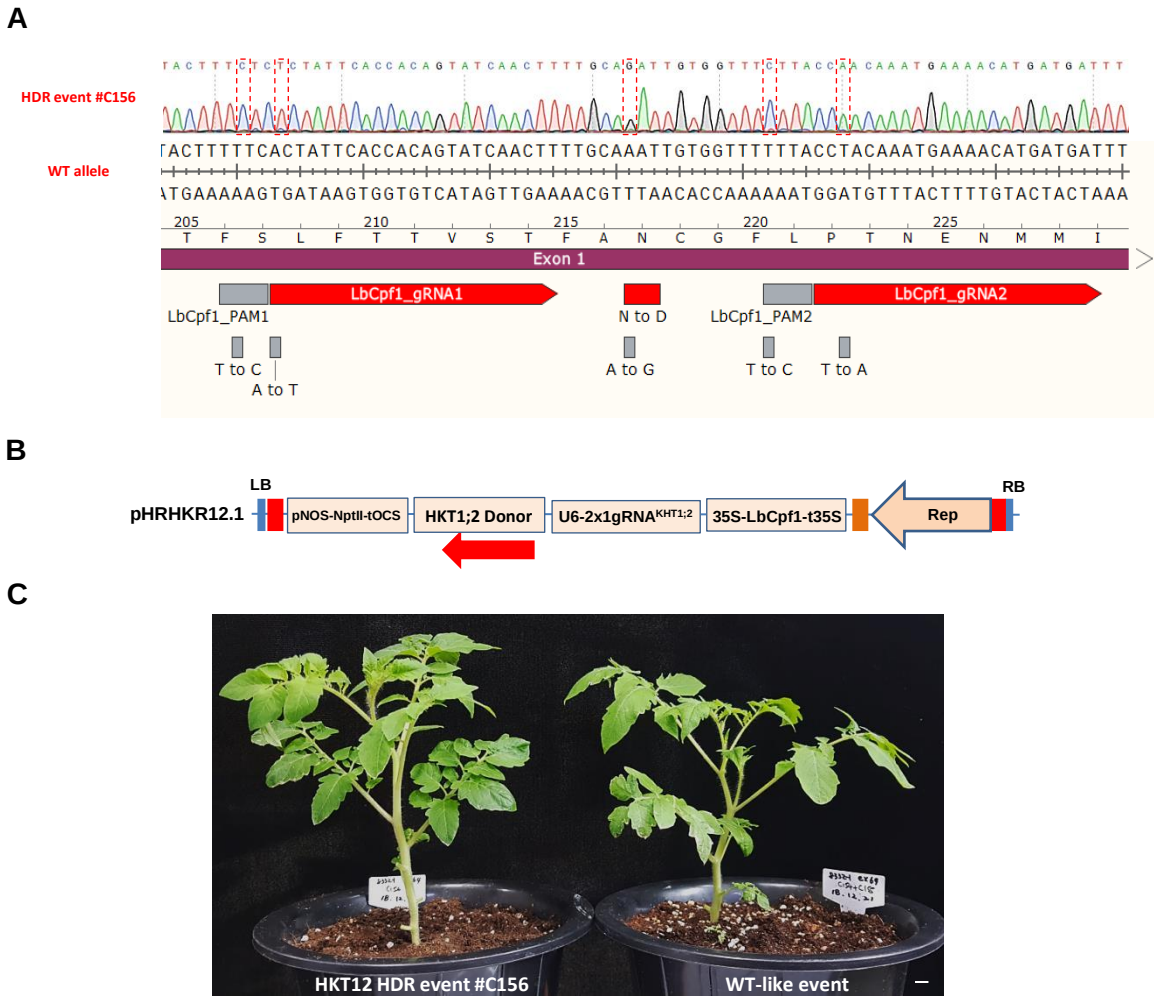

Figure 3. HKT1;2 N217D allele editing by HDR using the CRIPSR/Cpf1-based replicon system.
(**A**) Sanger sequencing of the event #C156 showing perfectly edited HKT1;2 N217 to D217 allele with WT allele as a reference. The nucleotides highlighted in the discontinuous red boxes denote intended modifications for N217D; PAM and core sequences (to avoid re-cutting).
(**B**) HDR construct layout for HKT1;2 editing. There is neither selection nor visible marker integrated into the donor sequence. The *Npt*II marker was used for enrichment of transformed cells.
(**C**) Morphology of the HKT1;2 N217D edited event compared to its parental WT in greenhouse conditions. Scale bar = 1 cm.

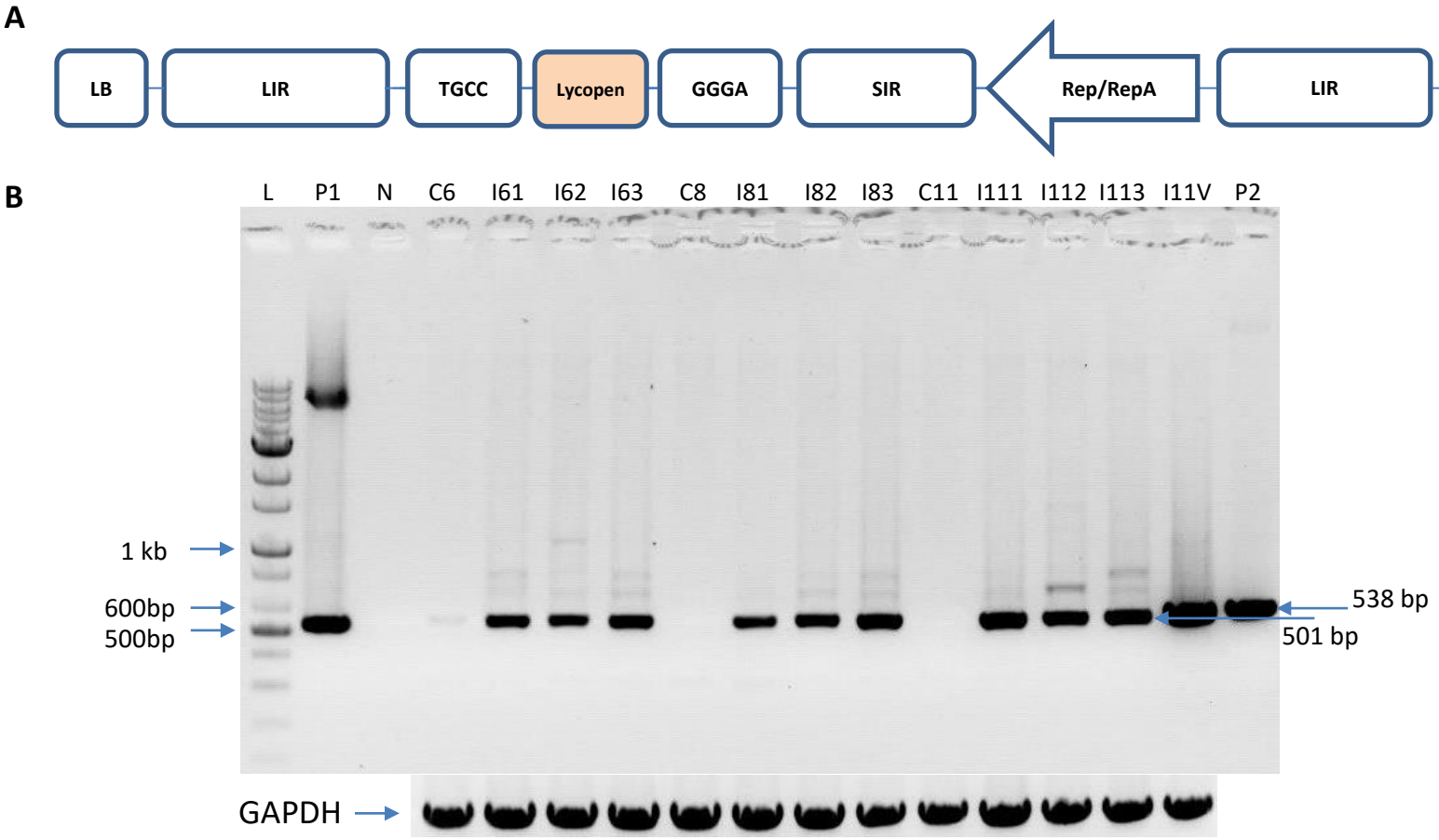

Supplemental Figure 1

The *de novo* engineered geminiviral amplicon (named as pLSL.R.Ly) and its replication in tomato.

(**A**) Map of pLSL.R.Ly. The DNA amplicon is defined by its boundary sequences (Long Intergenic Region, LIR) and a terminated sequence (Short Intergenic Region, SIR). The replication associated protein (Rep/RepA) is expressed from the LIR promoter sequence. All of the expression cassettes of HDR tools were cloned into the vector by replacing the red marker (Lycopene) using a pair of type IIS restriction enzyme (BpiI, flanking ends are TGCC and GGGA). Left (LB) and right (RB) denote the borders of a T-DNA. (**B**) Circulated DNA detection in tomato leaves infiltrated with pLSL.R.Ly compared to that of pLSLR. Agrobacteria containing the plasmids were infiltrated into tomato leaves (Hongkwang cultivar) and infiltrated leaf were collected at 6, 8 and 11 dpi and used for detection of circulated DNAs. N: water; P1: positive control for pLSL.R.Ly; positive control for P2: pLSLR; Cx: Control samples collected at x dpi; Ixy: infiltrated sample number y collected at x dpi; I11V: sample collected from leaves infiltrated with pLSLR at 11 dpi. PCRs using primers specific to GAPDH were used as loading control.

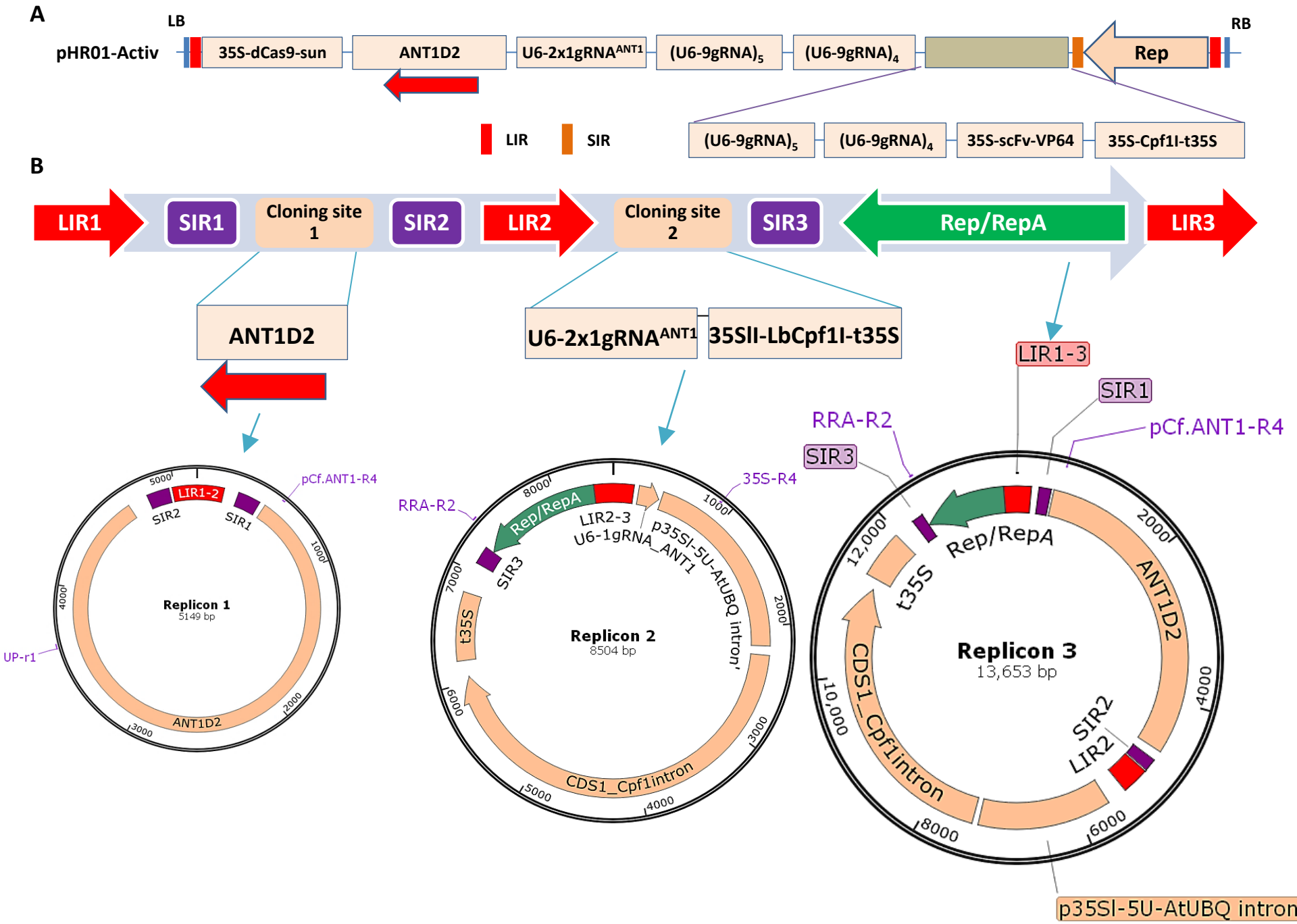
A
LB
RB
pHR01-Activ
35S-dCas9-sun
ANT1D2
U6-2x1gRNA^ANT1
(U6-9gRNA)5
(U6-9gRNA)4
Rep
LIR
SIR
(U6-9gRNA)5
(U6-9gRNA)4
35S-scFv-VP64
35S-Cpf1I-t35S
B
LIR1
SIR1
Cloning site 1
SIR2
LIR2
Cloning site 2
SIR3
Rep/RepA
LIR3
ANT1D2
U6-2x1gRNA^ANT1
35SII-LbCpf1I-t35S
LIR1-3
SIR1
pCf.ANT1-R4
RRA-R2
SIR3
35S-R4
Replicon 1
5149 bp
LIR1-2
SIR2
SIR1
pCf.ANT1-R4
UP-r1
ANT1D2
Replicon 2
8504 bp
RRA-R2
Rep/RepA
LIR2-3
U6-1gRNA_ANT1
p35SI-5U-AtUBQ intron'
35S-R4
SIR3
t35S
CDS1_Cpf1intron
Replicon 3
13,653 bp
Rep/RepA
t35S
ANT1D2
SIR2
LIR2
CDS1_Cpf1intron
p35SI-5U-AtUBQ intron

Supplemental Figure 2
Novel systems for HDR improvement.
(**A**) Single construct system for activation of HDR-related genes involving in HDR repair pathway. Long intergenic region (LIR) and short intergenic region (SIR) are depicted by color bars in the bottom. (**B**) Schematic system and released forms of multiple replicon system. General construction of multiple replicon complex is designed with 03 LIR and 03 SIR sequences (top panel). Donor template was cloned in one replicon and the other component for inducing DSBs were placed in the other replicon (middle panel). Three replicons would be formed from the construct (bottom panel).

HDR GE0 plant hardening in vermiculite pot

HDR GE0 plant in greenhouse conditions

Flowers of HDR GE0 compared to wildtype plant

Fruits of HDR plant event C1.4

Fruit slices of HDR plant Fruit of HDR GE0 vs. wildtype plant

Supplemental Figure 3
Morphological appearance of GE0 plants.

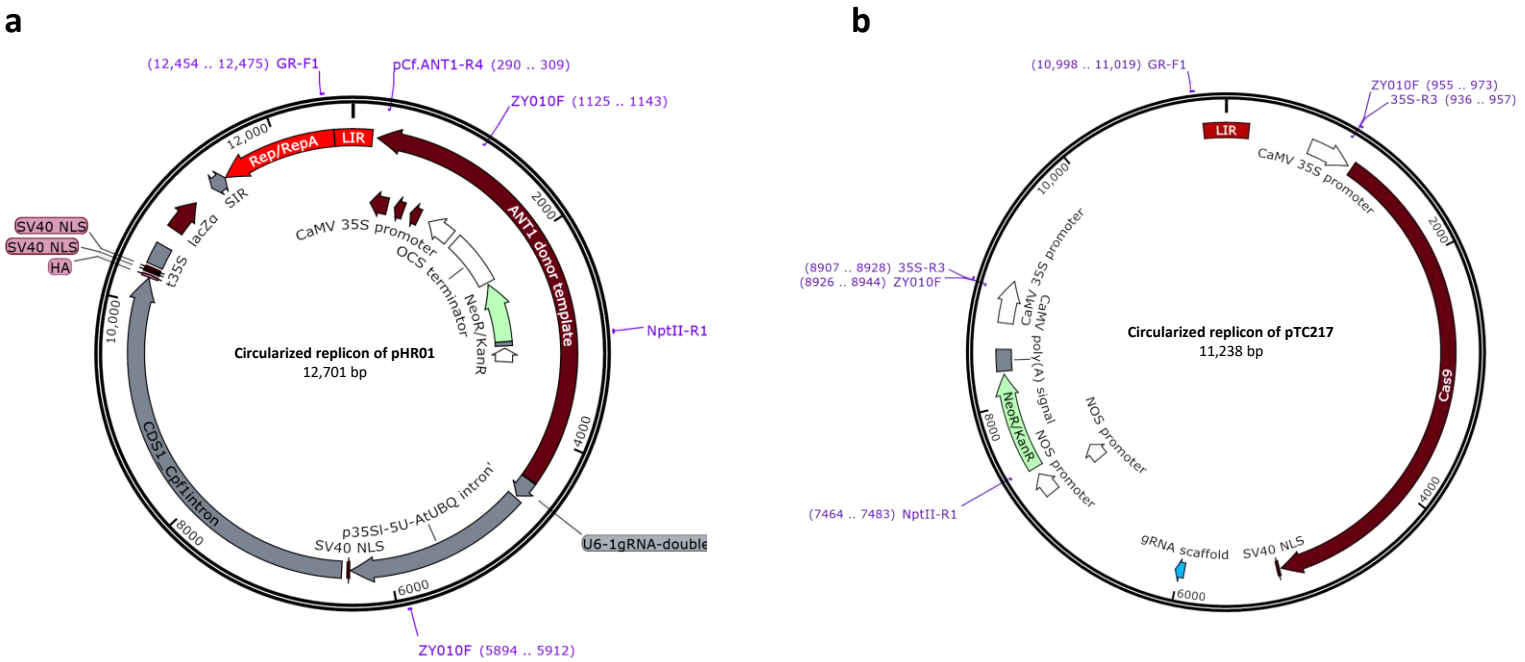

Supplemental Figure 4
Circularized DNA replicon released by HDR vectors.
(A) pHR01 replicon. (B) pTC217 replicon.

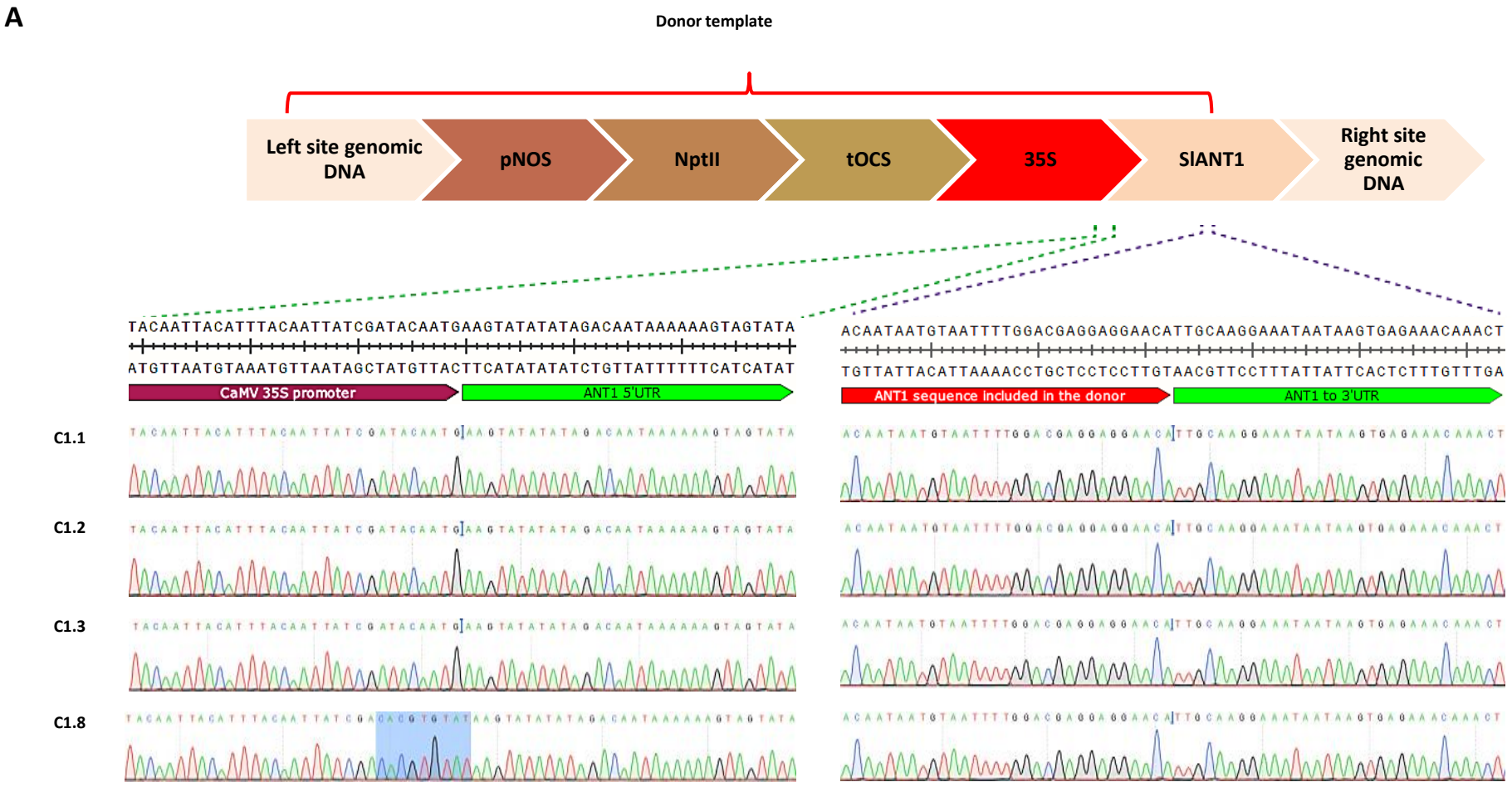

Supplemental Figure 5
Sanger sequencing data to confirm donor exchanges.
(**A**) Right junction.

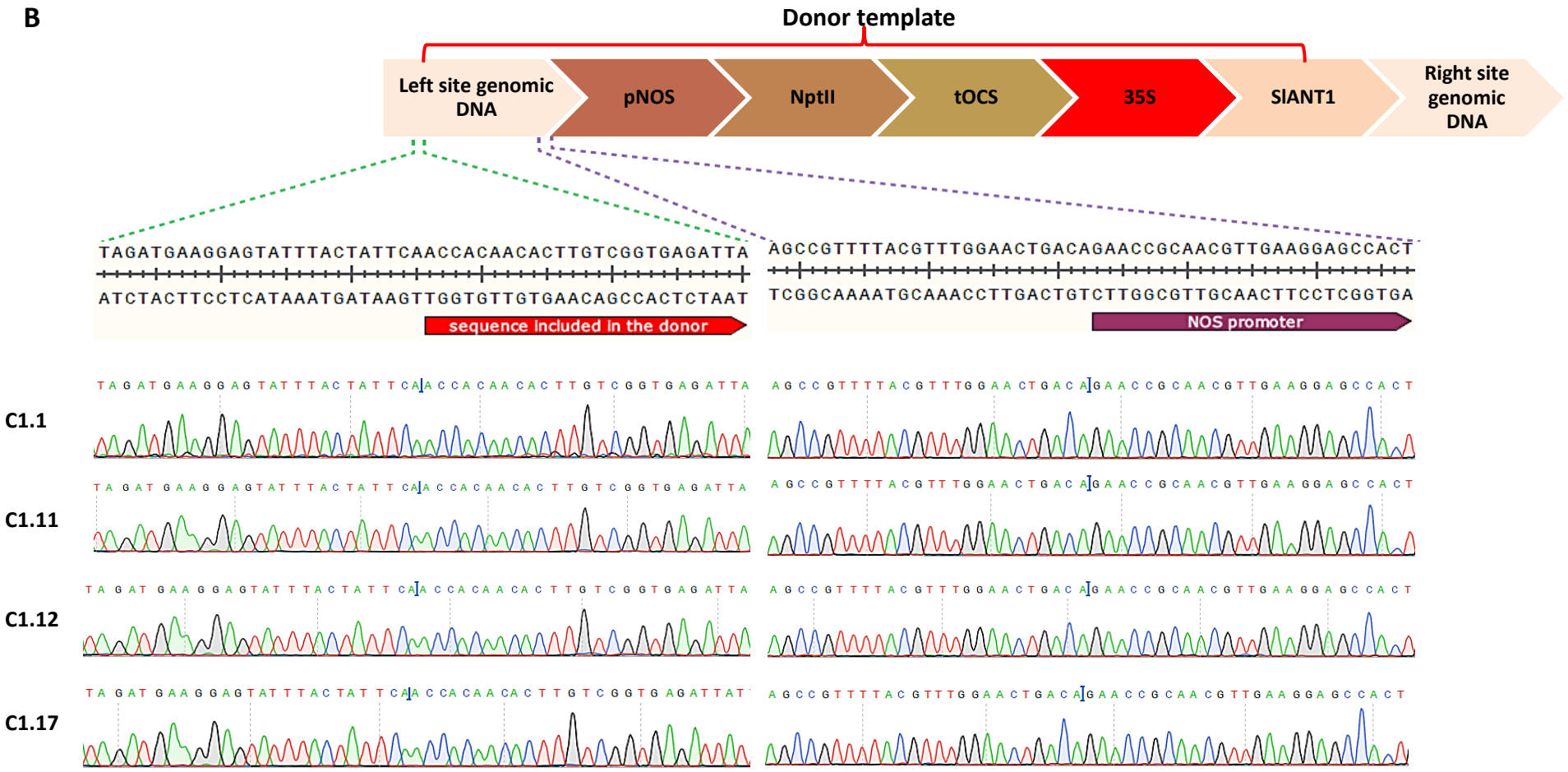

Supplemental Figure 5 (Continued)
Sanger sequencing data to confirm donor exchanges.
(**B**) Left junction. C1.1, C1.2, C1.3, C1.8, C1.11, C1.12, and C1.17: Independent LbCpf1-based HDR GE0 events

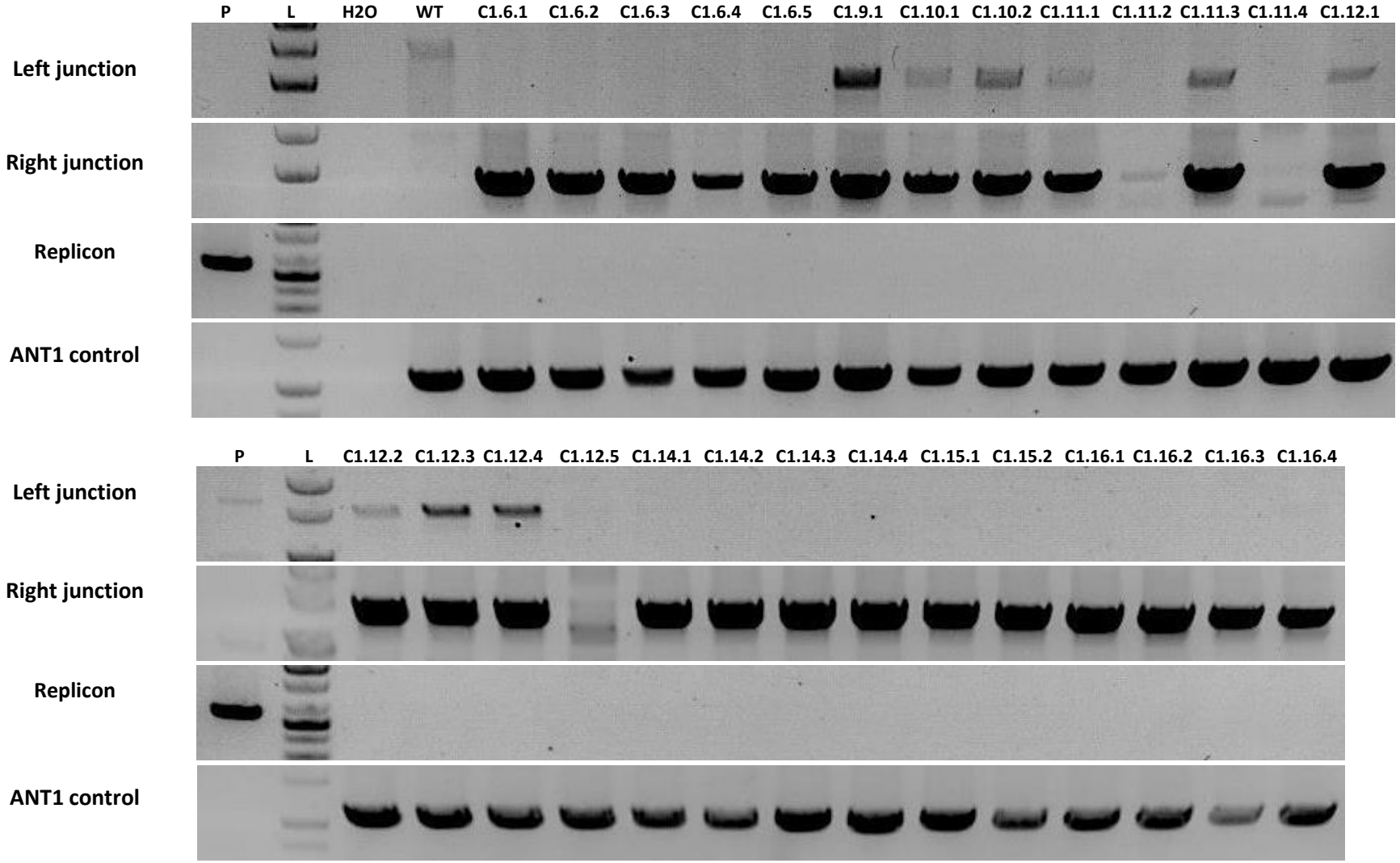

Supplemental Figure 6

PCR analyses of GE1 plants obtained from GE0 LbCpf1-based HR events .

P: pHR01 plasmid isolated from Agrobacteria; L: 1kb ladder; N: Water control; WT: wildtype Hongkwang; C1.6.1-C1.6.5: GE1 offspring of event #C1.6.; C1.9.1: GE1 offspring of event #C1.9; C1.10.1 and C1.10.2: GE1 offspring of event #C1.10; C1.11.1-C1.11.4: GE1 offspring of event #C1.11; C1.12.1-C1.12.5: GE1 offspring of event #C1.12; C1.14.1-C1.14.4: GE1 offspring of event #C1.14; C1.15.1 and C1.15.2: GE1 offspring of event #C1.15; C1.16.1-C1.16.4: GE1 offspring of event #C1.16.

Heterozygous HDR GE1 plant (htHDR)

Homozygous HDR GE1 plant (hmHDR)

Phenotypes of GE2 plants compared to WT. GE2 offspring (left) of hmHDR GE1 plant back-crossed with WT (middle) resulted in all htHDR BC1F1 plants

hmHDR

WT

htHDR

Supplemental Figure 7
Morphological appearance of GE1 plants

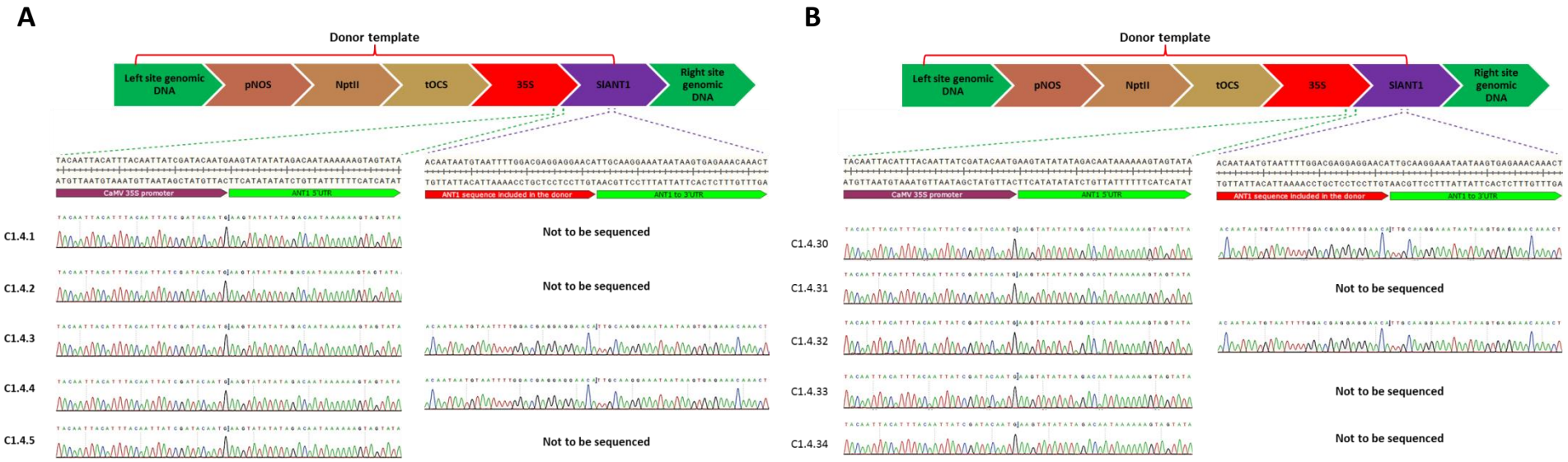

Supplemental Figure 8

Analyses of left and right junction sequences of GE1 plants.

Sanger sequencing data to confirm donor exchanges for right (**A**) and left (**B**) junctions of the GE1 plants are presented

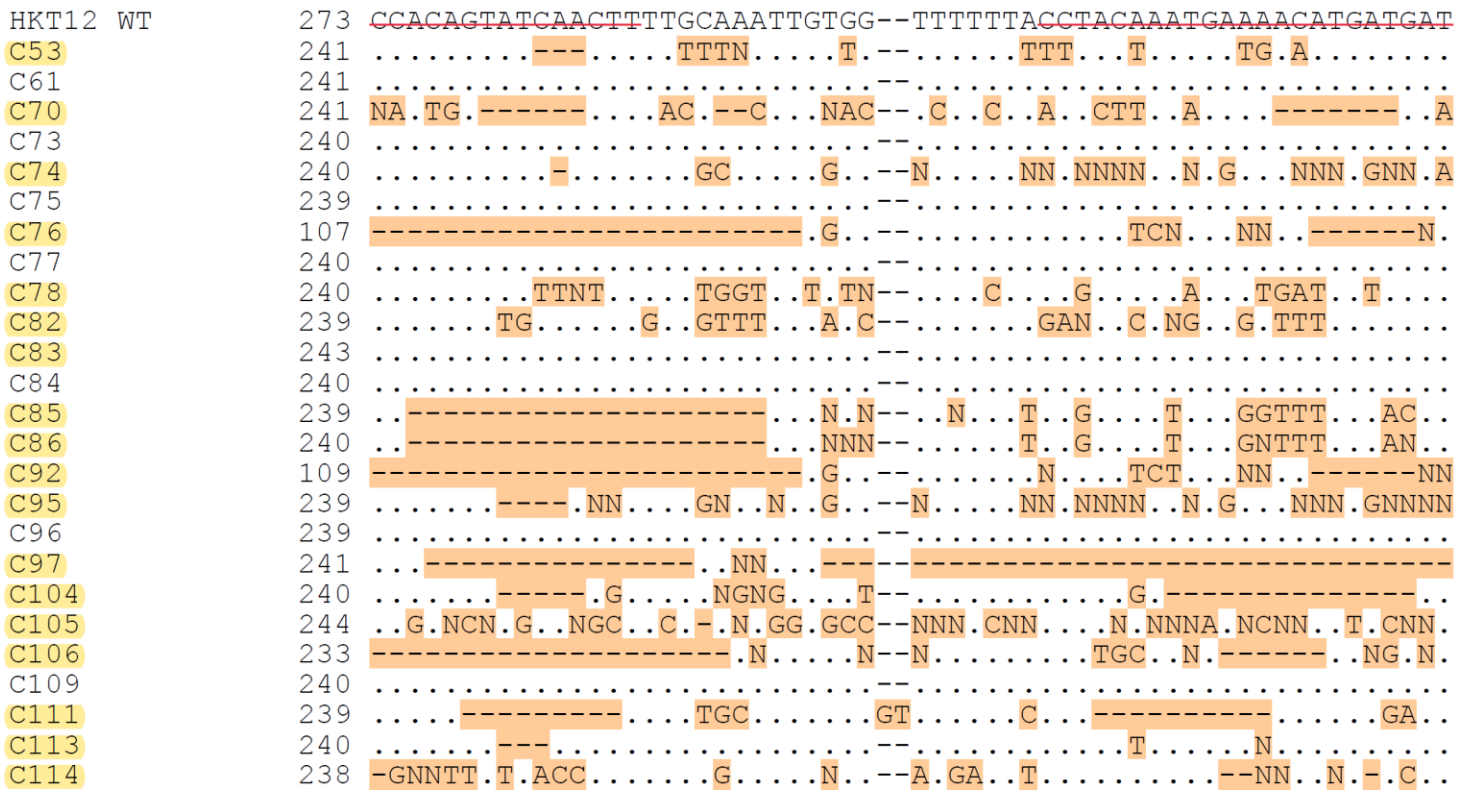

Supplemental Figure 9

Alignment of targeted regions isolated from the HKT12 events.

18/25 events (highlighted in yellow) showed strong double peaks indicating single/bi-allelic mutations. 6/25 events showed clearly bi-allelic mutations. C77 showed weak (30%) double peaks. C83 and C105 showed large truncations.

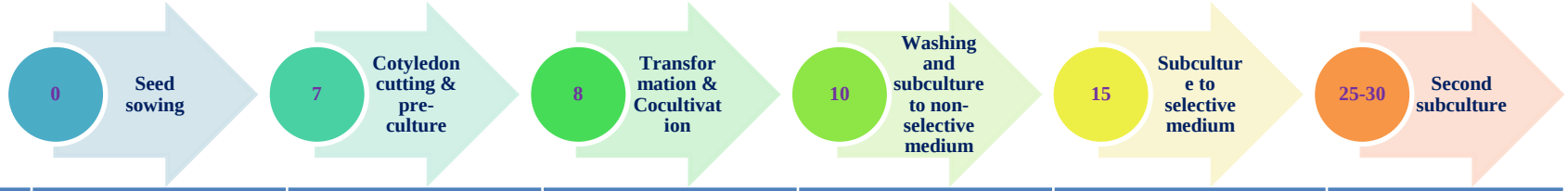

Stage	Germination	Pre-culture, calli induction	Co-cultivation, calli induction	Non-selection, calli induction	Selection, calli induction and shoot regeneration	Selection, shoot formation and elongation
Medium	MSO	PREMC,	ABM-MS	NSEL	SEL5	SEL5R
Temperature (°C)	25±2	25±1	25±1	31±1	28±1 for 5 days and then 25±2	25±2
Photoperiod	2 days-dark and then 16L/8D	1 day dark	2 days -dark	5 days-dark	5 days-8L/16D	16L/8D
Data collection	-	-	Sampling at 0dpt	Sampling at 3dpt and 6dpt	Sampling at 9dpt, Purple spot counting at 21 dpt	True shoot record

Supplemental Figure 10
Timeline and contents of *Agro*-mediated transformation protocol used in this work.
Step by step protocol is presented with each number in the circles indicates number of days after seed sowing (upper panel) and treatments used in each steps are shown in below panel.

Supplemental Table 1. Targeted genes and guide RNAs used in HDR activation experiment.

No.	Gene name	Accession number	Guide RNA1 sequence (5’-3’)	Guide RNA2 sequence (5’-3’)
1	SlMRE11	SL09G009340	ATCAAGTTAACGTTTATCTT	ATTAGAGATTATAAATTTAA
2	RAD51D	SL11G073220	TTTACAATAATATATAGTAA	AAGTTGTTAGCTAGAGTTTC
3	XRRC2	SL01G008520	TTTTAAAAGAAAAAATTAAA	ATACATATTTATGTTTGTTA
4	BRCA2	SL02G050200	TGCCCAACTAACGCTCAAAA	TGATAATAACAAAAATGACG
5	RAD54	SL04G056410	AAAAAAATTTGTATGTTGTT	TATTATTTTATGTTATTGTT
6	ATM	SL03G112940	TAGCATATGACCAAAATAAA	TAACAAAACAGAAAAAGAAG
7	RAD51	SL07G017540	ATGTGACCCAATACTTTAAG	TATACCCTTAAACTATATTC
8	RAD52-1	SL08G005060	TTCTATGCATAAATAATTAA	GAGAGAAAGAAGCCTCCTCA
9	RAD51B	SL11G072610	AGCTCTAAATGATAAAGTTG	

Supplemental Table 2. Primers for LbCpf1-based HR event analyses

No.	Product	Primer name	Sequence (5'-3')	Product length (bp)
1	Left junction	UPANT1-F1	TGCGATGATCTACGGTAACAAA	1485
2		NPTII-R1	GCGTGCAATCCATCTTGTTC	
3	Right junction	ZY010F	ACGTAAGGGATGACGCACA	1380
4		TC140R	TACCACCGGTCCATTCCCTA	
5	ANT1 control	TC140F	GGAAAATGGCATCTTGTTCCC	1056
6		TC140R	TACCACCGGTCCATTCCCTA	
7	Replicon	GR-F1	TTGAGATGAGCACTTGGGATAG	557
8		pCf.ANT1-R4	ACCTCAACGACGCAAGTATT	

Supplemental Table 3. Primers for SpCas9-based HR event analyses

No.	Product	Primer name	Sequence (5’-3’)	Product length (bp)
1	Left junction	UPANT1-F1	TGCGATGATCTACGGTAACAAA	1485
2		NPTII-R1	GCGTGCAATCCATCTTGTTC	
3	Right junction	ZY010F	ACGTAAGGGATGACGCACA	1380
4		TC140R	TACCACCGGTCCATTCCCTA	
5	ANT1 control	TC140F	GGAAAATGGCATCTTGTTCCC	1056
6		TC140R	TACCACCGGTCCATTCCCTA	
7	Replicon	GR-F1	TTGAGATGAGCACTTGGGATAG	1198
8		35S-R3	CGTCAGTGGAGATGTCACATCA	

Supplemental Table 4. Phenotypic segregation of self-pollinated offspring of the LbCpf1-based HDR events

No.	GE0 event	Total GE1 plants	Dark purple plant	hmHDR (%)*	Light purple plants	htHDR (%)**	WT-like	WT (%)
1	C1.4	113	30	26.5	37	32.7	46	40.7
2	C1.6	6	4	66.7	1	16.7	1	16.7
3	C1.9	1	1	100.0	0	0.0	0	0.0
4	C1.10	2	2	100.0	0	0.0	0	0.0
5	C1.11	10	5	50.0	4	40.0	1	10.0
6	C1.12	7	3	42.9	1	14.3	3	42.9
7	C1.14	4	4	100.0	0	0.0	0	0.0
8	C1.15	4	1	25.0	0	0.0	3	75.0
9	C1.16	7	3	42.9	2	28.6	2	28.6
Sum		154	53	34.4	45	29.2	56	36.4

*Dark purple or homozygous-like HDR plants
**Light purple or heterozygous-like HDR plants

Supplemental Table 5. Summary of SlHKT1;2 HDR experiment

Total number of seeds (at 70% germination rate)	Total cotyledon fragment	Total analyzed events	Total Potential HDR events	Total true HDR events	HDR efficiency
460	640*	150	09	01	0.66%**

*Can be done in only one transformation.
**HKT1;2 gene donor template contains neither antibiotic selection marker nor ANT1 color marker.